Applied Mathematics Letters 142 (2023) 108641

Contents lists available at ScienceDirect

Applied Mathematics Letters

www.elsevier.com/locate/aml

A first-order stabilization-free Virtual Element Method

Stefano Berrone[1], Andrea Borio[1], Francesca Marcon*[,1], Gioana Teora[1]

Dipartimento di Scienze Matematiche, Politecnico di Torino, Corso Duca degli Abruzzi 24, Torino, 10129, Italy

ARTICLE INFO

Article history:
Received 31 December 2022
Received in revised form 6 March 2023
Accepted 6 March 2023
Available online 14 March 2023

Keywords:
Virtual Element Method
Stabilization-free
Polygonal meshes

ABSTRACT

In this paper, we introduce a new Virtual Element Method (VEM) not requiring any stabilization term based on the usual enhanced first-order VEM space. The new method relies on a modified formulation of the discrete diffusion operator that ensures stability preserving all the properties of the differential operator.

1. Introduction

Recently, in the context of Virtual Element Methods (VEM), a growing interest has been devoted to the definition of bilinear forms not requiring a stabilization term. In [1], a lowest-order stabilization-free scheme was proposed and analysed, proving that it is possible to define coercive bilinear forms based on polynomial projections of virtual basis functions of suitable high-degree polynomial spaces. In [2], the proposed scheme was compared to standard VEM, and results showed that the absence of a stabilization operator can reduce the error and help convergence in case of strongly anisotropic problems.

In this paper, we propose a variation of the scheme introduced in [1], strongly exploiting the theory developed in that paper to choose the smallest possible polynomial space that guarantees coercivity.

We consider an open bounded domain $\Omega \subset \mathbb{R}^2$ and the following standard advection–diffusion–reaction problem: *find* $u \in \mathrm{H}_0^1(\Omega)$ *such that*

$$(\mathcal{K}\nabla u, \nabla v)_\Omega + (\boldsymbol{\beta} \cdot \nabla u, v)_\Omega + (\gamma u, v)_\Omega = (f, v)_\Omega \quad \forall v \in \mathrm{H}_0^1(\Omega)\,, \tag{1}$$

* Corresponding author.
E-mail addresses: stefano.berrone@polito.it (S. Berrone), andrea.borio@polito.it (A. Borio), francesca.marcon@polito.it (F. Marcon), gioana.teora@polito.it (G. Teora).

1 The authors are members of the INdAM-GNCS. The authors S.B. and A.B. kindly acknowledge partial financial support provided by INdAM-GNCS Projects 2022 and 2023, by the MIUR project “Dipartimenti di Eccellenza” Programme (2018–2022) CUP:E11G18000350001 and by the PRIN 2020 project (No. 20204LN5N5_003). The authors S.B, A.B and F.M. kindly acknowledge financial support provided by PNRR M4C2 project of CN00000013 National Centre for HPC, Big Data and Quantum Computing (HPC) CUP:E13C22000990001. The author G.T. kindly acknowledge financial support provided by the MIUR programme “Programma Operativo Nazionale Ricerca e Innovazione 2014–2020” (CUP: E11B21006490005).

https://doi.org/10.1016/j.aml.2023.108641
0893-9659/

where $(\cdot,\cdot)_{\Omega}$ denotes the $\mathrm{L}^2(\Omega)$ scalar product. We make standard assumptions on the coefficients in order to guarantee the well-posedness of the problem, namely, all coefficients are $\mathrm{L}^\infty(\Omega)$, $\mathcal{K}$ is a symmetric uniformly positive definite tensor, $\operatorname{div}\boldsymbol{\beta}=0$, and $\inf_{x\in\Omega}\gamma(x)\geq 0$. Here we consider homogeneous Dirichlet boundary conditions, but more general boundary conditions can be considered.

2. Local spaces and projections

We consider a family of polygonal tessellations $\mathcal{M}_h$ of Ω, satisfying the following standard mesh assumptions: $\exists\kappa>0$ such that $\forall E\in\mathcal{M}_h$, E is star-shaped with respect to a ball of radius $\rho\geq\kappa h_E$, and $\forall e\in\mathcal{E}_E$, where $\mathcal{E}_E$ is the set of edges of E, $|e|\geq\kappa h_E$, where h_E denotes the diameter of E. For any given $E\in\mathcal{M}_h$, we define the following standard Virtual Element space [3]:

$$\mathcal{V}_h^E=\Big\{v\in\mathrm{H}^1(E)\colon \Delta v\in\mathbb{P}_1(E)\,,\ \gamma^{\partial E}(v)\in C^0(\partial E)\,,\gamma^e(v)\in\mathbb{P}_1(e)\ \forall e\in\mathcal{E}_E,\\ \left(v-\Pi_1^{\nabla,E}v,p\right)_E=0\ \forall p\in\mathbb{P}_1(E)\Big\}\,,$$

where $\gamma^\omega(v)$ denotes the trace of v on ω and $\Pi_1^{\nabla,E}v\in\mathbb{P}_1(E)$ is defined such that $\left(\nabla v-\nabla\Pi_1^{\nabla,E}v,\nabla p\right)_E=0$ $\forall p\in\mathbb{P}_1(E)$ and $\int_{\partial E}v=\int_{\partial E}\Pi_1^{\nabla,E}v$. The degrees of freedom of $\mathcal{V}_h^E$ are the values of functions at the vertices of the polygon E.

For any given $\ell\in\mathbb{N}$, we define the following spaces of harmonic polynomials of degree $\ell+1$:

$$\mathbb{H}_{\ell+1}(E)=\left\{p\in\mathbb{P}_{\ell+1}(E):\Delta p=0,\int_E p=0\right\}.$$

Let $\nabla\mathbb{H}_{\ell+1}(E)$ be the space of gradients of functions in $\mathbb{H}_{\ell+1}(E)$. We define the projector $\Pi_\ell^{\mathbb{H},E}\colon\left[\mathrm{L}^2(E)\right]^2\to\nabla\mathbb{H}_{\ell+1}(E)$ such that, $\forall\boldsymbol{v}\in\left[\mathrm{L}^2(E)\right]^2$,

$$\left(\Pi_\ell^{\mathbb{H},E}\boldsymbol{v},\nabla p_{\ell+1}\right)_E=(\boldsymbol{v},\nabla p_{\ell+1})_E\quad\forall p_{\ell+1}\in\mathbb{H}_{\ell+1}(E)\,. \tag{2}$$

Notice that, since $\mathbb{H}_{\ell+1}(E)$ does not contain constants by definition, $\nabla p_{\ell+1}$ is never zero in (2) and $\dim\nabla\mathbb{H}_{\ell+1}(E)=\dim\mathbb{H}_{\ell+1}(E)=2\ell+2$. Moreover, notice that $[\mathbb{P}_0(E)]^2\subseteq\nabla\mathbb{H}_{\ell+1}(E)$, and in particular $[\mathbb{P}_0(E)]^2=\nabla\mathbb{H}_1(E)$.

Now, given a function $v_h\in\mathcal{V}_h^E$, consider the problem of computing $\Pi_\ell^{\mathbb{H},E}\nabla v_h$. Let $\{h_i, i=1,\dots,2\ell+2\}$ be a set of basis functions of $\mathbb{H}_{\ell+1}(E)$. Then $\Pi_\ell^{\mathbb{H},E}\nabla v_h=\sum_{j=1}^{2l+2}d_j\nabla h_j$, where the values d_j can be computed by solving the following system of equations:

$$\sum_{j=1}^{2l+2}(\nabla h_j,\nabla h_i)_E\,d_j=(\nabla v_h,\nabla h_i)_E\quad\forall i=1,\dots,2\ell+2\,. \tag{3}$$

The right-hand side can be computed since we know v_h analytically on the boundary, recalling that $\Delta h_i=0$ and applying Green's theorem: $(\nabla v_h,\nabla h_i)_E=\left(v_h,\frac{\partial h_i}{\partial n}\right)_{\partial E}$, $\forall i=1,\dots,2\ell+2$. On each edge, the right-hand side is the integral of a polynomial of degree $\ell+1$, that can be computed exactly using $\lceil\frac{\ell+2}{2}\rceil$ Gauss quadrature nodes. Concerning the left-hand side of (3), a way to reduce the computational cost, with respect to 2D quadrature rules, is to observe that $(\nabla h_j,\nabla h_i)_E=\left(h_j,\frac{\partial h_i}{\partial n}\right)_{\partial E}$, that is the integral of a piecewise polynomial of degree $2\ell+1$. Then, the integral can be computed by $\ell+1$ Gauss quadrature nodes on each edge, reducing the number of function evaluations to $\sim N_E\ell$.

3. Discrete variational formulation

Let $\mathcal{V}_h = \{v_h \in \mathrm{H}^1_0(\Omega) : v_h \in \mathcal{V}_h^E \ \forall E \in \mathcal{M}_h\}$ and let $\ell_E \geq 0$ be given $\forall E \in \mathcal{M}_h$, possibly different from one polygon to another. Then, we look for $u_h \in \mathcal{V}_h$ such that

$$\begin{aligned}\sum_{E\in\mathcal{M}_h} &\left(\mathcal{K}\Pi^{\mathbb{H},E}_{\ell_E}\nabla u_h, \Pi^{\mathbb{H},E}_{\ell_E}\nabla v_h\right)_E + \left(\boldsymbol{\beta}\cdot\Pi^{\mathbb{H},E}_{\ell_E}\nabla u_h, \Pi^{0,E}_0 v_h\right)_E \\ &+ \left(\gamma\Pi^{0,E}_0 u_h, \Pi^{0,E}_0 v_h\right)_E = \sum_{E\in\mathcal{M}_h}\left(f, \Pi^{0,E}_0 v_h\right)_E \quad \forall v_h \in \mathcal{V}_h\,,\end{aligned} \tag{4}$$

where $\Pi^{0,E}_0$ is the L^2 projection operator onto constants. The following result provides the crucial ingredient for the well-posedness of (4).

Theorem 1. *Assume that, $\forall E \in \mathcal{M}_h$, $2\ell_E + 2 \geq N_E - 1$, N_E being the number of vertices of E. Then there exist $\alpha^*, \alpha_* > 0$, depending on the mesh regularity parameter κ and on local variations of $\mathcal{K}$, such that, $\forall u_h \in \mathcal{V}_h$, $\forall E \in \mathcal{M}_h$,*

$$\alpha_* \left\|\sqrt{\mathcal{K}}\nabla u_h\right\|_E \leq \left\|\sqrt{\mathcal{K}}\Pi^{\mathbb{H},E}_{\ell_E}\nabla u_h\right\|_E \leq \alpha^* \left\|\sqrt{\mathcal{K}}\nabla u_h\right\|_E .$$

Proof. The result follows from the theory developed in [1]. □

Theorem 1 provides us a sufficient condition for the coercivity of the diffusivity term of (4). The well-posedness of the discrete problem is then obtained by the same arguments as in [3]. Optimal order a priori error estimates can be proved using the techniques in [1,3]. In particular, we get

$$\left\|\sqrt{\mathcal{K}}\nabla(u - u_h)\right\|_\Omega = O(h)\,, \qquad \|u - u_h\|_\Omega = O(h^2).$$

Remark 1. A basis of the space of harmonic polynomials of degree $\ell + 1$ is known in closed form and is given by the recurrence relation (see [4]). Notice that the requirement of zero integral in $\mathbb{H}_{\ell+1}(E)$ can be disregarded in practice, since enforcing zero integral into basis functions would not change the results of the required computations.

4. Numerical results

In this section, we propose some numerical experiments to validate our method. We first give numerical evidence of the coercivity of our local bilinear form, then we present some convergence tests that assess the theoretical estimates and compare the errors

$$e_0 = \frac{\sqrt{\sum_{E\in\mathcal{T}_h}\left\|u - \Pi^{\nabla,E}_1 u_h\right\|^2_E}}{\|u\|_\Omega}, \quad e_1 = \frac{\sqrt{\sum_{E\in\mathcal{T}_h}\left\|\sqrt{\mathcal{K}}\left(\nabla u - \nabla\Pi^{\nabla,E}_1 u_h\right)^2\right\|_E}}{\left\|\sqrt{\mathcal{K}}\nabla u\right\|_\Omega}, \tag{5}$$

with respect to the one made by the standard Virtual Element Method [5].

In the first test, we consider a set of different polygons, with different geometrical features, such as concavities, symmetries, and aligned edges. For each polygon, choosing ℓ_E according to Theorem 1, we assess the local stability of the discrete diffusion operator (4) ($\mathcal{K} = 1$, $\boldsymbol{\beta} = 0$, and $\gamma = 0$), evaluating the second smallest singular value of the elemental stiffness matrix denoted by σ_r. The results, reported in Table 1, confirm the stability of the method and good robustness with respect to the geometrical complexity being

Table 1
σ_r of the elemental stiffness matrices related to different kinds of polygons.

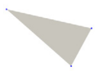		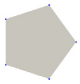		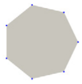	
Irregular	Concave	Regular	Irregular with hanging nodes	Regular	Star
$N_E = 3$, $\ell_E = 0$	$N_E = 4$, $\ell_E = 1$	$N_E = 5$, $\ell_E = 1$	$N_E = 6$, $\ell_E = 2$	$N_E = 7$, $\ell_E = 2$	$N_E = 8$, $\ell_E = 3$
$\sigma_r = 3.8227e\text{-}01$	$\sigma_r = 1.9207\text{-}01$	$\sigma_r = 7.1889e\text{-}01$	$\sigma_r = 1.6542e\text{-}01$	$\sigma_r = 6.6611e\text{-}01$	$\sigma_r = 2.0525e\text{-}01$
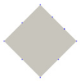	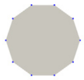	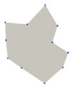	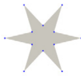	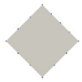	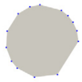
Irregular with hanging nodes	Regular	Concave	Star	Irregular with hanging nodes	Irregular
$N_E = 9$, $\ell_E = 3$	$N_E = 10$, $\ell_E = 4$	$N_E = 11$, $\ell_E = 4$	$N_E = 12$, $\ell_E = 5$	$N_E = 13$, $\ell_E = 5$	$N_E = 14$, $\ell_E = 6$
$\sigma_r = 2.4452e\text{-}01$	$\sigma_r = 5.8778e\text{-}01$	$\sigma_r = 1.1917e\text{-}01$	$\sigma_r = 1.0911e\text{-}01$	$\sigma_r = 1.5378e\text{-}01$	$\sigma_r = 4.8291e\text{-}02$
	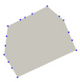			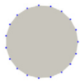	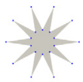
Regular	Irregular with hanging nodes	Concave	Irregular with a collapsing edge	Regular	Star
$N_E = 15$, $\ell_E = 6$	$N_E = 16$, $\ell_E = 7$	$N_E = 17$, $\ell_E = 7$	$N_E = 18$, $\ell_E = 8$	$N_E = 19$, $\ell_E = 9$	$N_E = 20$, $\ell_E = 10$
$\sigma_r = 4.0674e\text{-}01$	$\sigma_r = 1.3047e\text{-}04$	$\sigma_r = 1.1031e\text{-}02$	$\sigma_r = 2.3334e\text{-}02$	$\sigma_r = 3.2470e\text{-}01$	$\sigma_r = 3.6314e\text{-}02$

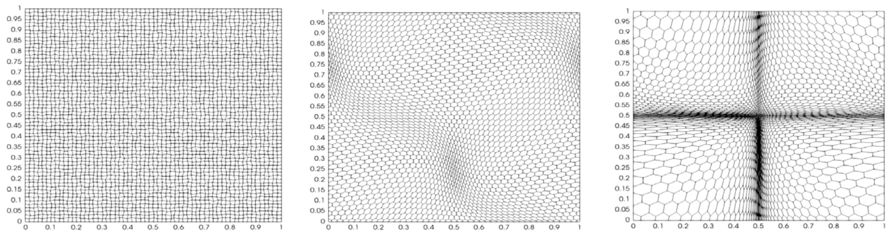

(a) (b) (c)

Fig. 1. Meshes used in the numerical experiments. Left: Distorted squared mesh. Center: Distorted Voronoi mesh. Right: Highly-distorted Voronoi mesh.

σ_r always well detached from zero, i.e. substantially distant from the machine precision (the smallest singular value of the elemental stiffness matrix is always vanishing).

In the second test, we compare the stabilization-free Virtual Element Method (SFVEM in short) with the standard VEM with the *dofi-dofi* stabilization term (VEM in short) [3] by plotting the relative errors e_0 and e_1 (5), and computing their rates of convergence on three families of distorted and highly-distorted meshes. The fourth refinement of each family of meshes is shown in Fig. 1. Before performing the comparison, we analyse the minimum σ_r, as in Table 1, over the polygons of each family of meshes. We obtain $\sigma_r = 4.97\text{e}{-}01$ for the distorted squared mesh Fig. 1(a), $\sigma_r = 7.02\text{e}{-}02$ and $\sigma_r = 7.16\text{e}{-}03$ for the distorted Voronoi mesh Fig. 1(b) and the highly-distorted Voronoi mesh Fig. 1(c), respectively. In order to show the advantages of SFVEM with respect to the standard VEM, as suggested in [2], we consider an *anisotropic* diffusion tensor $\mathcal{K}$. Let Ω be the unit square, we consider the advection–diffusion–reaction problem (1) with coefficients

$$\mathcal{K} = \mathbf{G} \begin{bmatrix} 1 & 0 \\ 0 & 1.0e\text{-}09 \end{bmatrix} \mathbf{G}^T, \quad \mathbf{G} = \begin{bmatrix} \cos(\theta) & -\sin(\theta) \\ \sin(\theta) & \cos(\theta) \end{bmatrix}, \quad \boldsymbol{\beta}(x,y) = \begin{bmatrix} \boldsymbol{\beta}_1(x,y) \\ \boldsymbol{\beta}_2(x,y) \end{bmatrix},$$

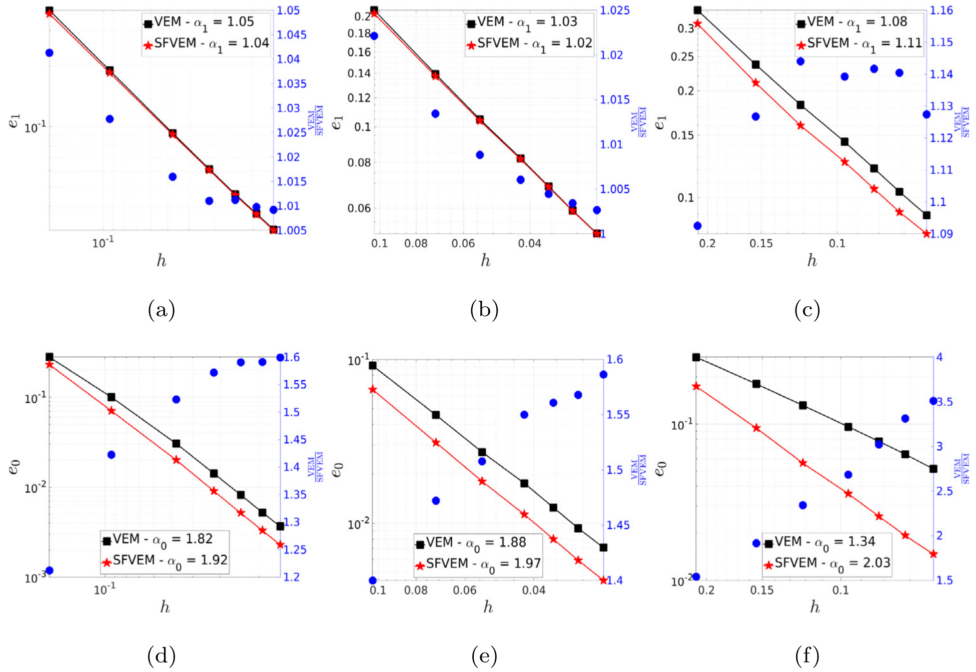

Fig. 2. Behaviour of errors e_0 and e_1 (5) w.r.t. h. First column: Distorted squared mesh. Second column: Distorted Voronoi mesh. Last column: Highly-distorted Voronoi mesh.

and $\gamma(x, y) = x(1-x)y(1-y)$, where $\mathbf{G}$ is the Givens rotation matrix with $\theta \in \mathbb{R}$. For R_1, $R_2 \in [0, 1]$, we define [6]

$$\begin{aligned}
\boldsymbol{\beta}_1(x, y; R_1) &= 250000x^4y^3(R_1 - x)(1-x)^4 \\
&\qquad \left[4R_2\left(1 - 5y + 9y^2 - 7y^3 + 2y^4\right) - 5y + 24y^2 - 42y^3 + 32y^4 - 9y^5\right], \\
\boldsymbol{\beta}_2(x, y; R_2) &= -\boldsymbol{\beta}_1(y, x; R_2),
\end{aligned}$$

and we fix $R_1 = 0.9$, $R_2 = 0.3$ and $\theta = \frac{\pi}{6}$. We choose $f(x, y)$ in such a way the exact solution is $u(x, y) = \boldsymbol{\beta}_1(x, y)$.

In Fig. 2, we plot the convergence curves of errors e_0 and e_1 (5) and the ratio between their values for VEM and SFVEM (right axis of each figure). The legends report the rates of convergence of the errors (α_0 and α_1, respectively). The performances of the two methods are almost equivalent concerning the e_1 error, see Figs 2(a)–2(c). Whereas in Figs 2(d)–2(f) SFVEM easily reaches the asymptotic rates of convergence on all the meshes and displays a smaller e_0 error, whereas VEM is still in a pre-asymptotic regime on highly-distorted Voronoi meshes and displays an error between two and three times w.r.t. SFVEM.

5. Conclusion

We propose a new first-order stabilization-free VEM that exploits projections on harmonic polynomials to build a self-stabilized bilinear form. We modify the polynomial projection proposed in [1], strongly exploiting theoretical results presented in that paper, in order to construct the smallest possible polynomial space that ensures coercivity of the induced bilinear form. Numerical results show good stability of the method and optimal rates of convergence.

Data availability

Data will be made available on request.

References

[1] S. Berrone, A. Borio, F. Marcon, Lowest order stabilization free virtual element method for the 2D Poisson equation, 2021, arXiv:2103.16896.
[2] S. Berrone, A. Borio, F. Marcon, Comparison of standard and stabilization free virtual elements on anisotropic elliptic problems, App. Math. Lett. 129 (2022) 107971.
[3] L. Beirão da Veiga, F. Brezzi, L.D. Marini, A. Russo, Virtual element methods for general second order elliptic problems on polygonal meshes, Math. Models Methods Appl. Sci. 26 (04) (2015) 729–750.
[4] J.B. Perot, C. Chartrand, A mimetic method for polygons, J. Comput. Phys. 424 (C) (2021) 109853.
[5] L. Beirão da Veiga, G. Manzini, Residual a posteriori error estimation for the virtual element method for elliptic problems, ESAIM: M2AN 49 (2) (2015) 577–599.
[6] S. Berrone, Robustness in a posteriori error estimates for the oseen equations with general boundary conditions, in: Numerical Mathematics and Advanced Applications, Springer Milan, 2003, pp. 657–668.